Journal of Metals, Materials and Minerals, 33(4), 1723, 2023

Microstructure and mechanical properties of 0.2C-3.9Al-1.12Mn-0.3Mo δ-TRIP steel as a function of isothermal bainitic transformation temperature

Mahsa GHOLAMBARGANI[1], Yahya PALIZDAR[1,*], and Ali KHANLAKHANI[1]

[1] *Nanotechnology and Advanced Materials Department, Materials and Energy Research Center, Karaj, Iran*

***Corresponding author e-mail:** y.palizdar@merc.ac.ir

Received date:
1 May 2023
Revised date
18 August 2023
Accepted date:
25 August 2023

Keywords:
δ-TRIP steel;
Bainitic transformation process;
Retained austenite;
TRIP-assisted steel;
TRIP effect

Abstract

The present investigation employed a two-stage heat treatment on a δ-transformation-induced plasticity (TRIP) steel comprising 0.2C–4Al–1.2Mn–0.3Mo (wt%). The mechanical and microstructural characteristics that result from varied isothermal bainitic transformation (IBT) temperatures following inter-critical annealing at 820°C for 10 min are thoroughly analyzed. The microstructure of the steels consisted of δ-ferrite, α-ferrite, bainitic ferrite, retained austenite (RA), and martensite, resulting in an optimum combination of the ultimate tensile strength (UTS) and total elongation (TE). The results of the investigation showed that IBT temperature had an effect on the stability of RA and the martensitic transition. Due to the increased mechanical stability of RA, the study revealed that the TRIP phenomenon was more prominent at lower IBT temperatures. Both tensile and yield strengths, as well as elongation, decreased as a consequence of the increase in IBT temperature. Maximum values of UTS, TE, and the product of these two properties (PSE) are attained (860 MPa, 41%, and 35260 MPa·%, respectively) under optimal processing conditions (at 350°C IBT temperature in 10 min).

1. Introduction

In order to produce lightweight steels for vehicle bodies in response to simultaneously higher mechanical characteristics and lowered pricing [1-4], active research is being conducted on the TRIP-assisted steels that include multiphase microstructure. Zackay and colleagues [5] were the ones who made the discovery of transformation-induced plasticity (TRIP) steels, which is widely known. After that, in 1987, Matsmura discovered TRIP-assisted steels that have between 50% and 60% allotropic ferrite, between 20% and 30 % bainite ferrite without carbide, and retained austenite (RA) with high carbon [6], all of which are of good quality and have a low cost. The scientific community as well as industry has noted an increasing interest in TRIP-assisted steels. Low carbon and low alloy TRIP-assisted steels often have a complex microstructure that consists of both ductile phase (austenite) and high strength (martensite) phases. In most cases, the matrix structure of TRIP-assisted steel is what determines the strength of the steel [7-10]. Through external stress, the metastable RA dispersed between the bainite laths might convert into martensite. The TRIP effect is a phenomenon that increases plastic deformation and toughness while simultaneously increasing steel strength [4,11-13].

This microstructure of TRIP-assisted steel consists of many different phases and is often the result of a two-stage heat treatment. The two-stage process includes inter-critical annealing (ICA) followed by austempering at the bainite transition temperature [14-17]. The second phase sometimes called the isothermal bainitic transformation (IBT), starts after the previous one ends. In the second step, pearlite production is prevented by rapidly cooling TRIP steels to the bainite reaction temperature range and maintaining them at that temperature.

To achieve superior mechanical properties, high-Al TRIP-assisted (δ-TRIP) steel relies heavily on its alloying elements. In addition, it is generally agreed that a significant amount of RA in these steels may be attributed to the presence of Al in the chemical composition [18]. In all solid states, the presence of Al up to 1.5 wt% is shown by Yi *et al*. [19] to be a stabilizing element of the δ-ferrite, which contributes to excellent tensile properties. Additional factors that contribute to RA's stability include carbon and grain size. That is because there are not as many places for nucleation to occur during the martensite transformation [2,20].

The mechanical properties of steels with δ-ferrite phase are uncertain [21,22]. Due to its inconsistency with the matrix and its change to brittle intermetallic phase or carbides at high temperatures, δ-ferrite can decrease mechanical qualities. Other studies, on the other hand, have demonstrated that δ-ferrite may improve the ductility and/or toughness of martensitic steel, resulting in greater resistance to stress corrosion cracking [23]. It has also been observed that the morphology of δ-ferrite, specifically a bamboo-like form of δ-ferrite that runs parallel to the loading direction, is essential for boosting the creep resistance of the material.

Numerous publications on the impact of alloying elements [24,27], initial and assessed microstructure [28-30], heat-treatment techniques [19,23], and heating rate on the microstructure and mechanical characteristics have been published in this field. Maintaining the chosen temperature during the IBT stage for an appropriate amount of

time may guarantee the development of bainite and the carbon enrichment of RA. As a practical matter, what is ultimately created as a consequence of this process is austenite in the form of a multiphase structure [23].

The exceptional potential of δ-TRIP steel as a groundbreaking automotive material lies in its remarkable strength, formability, and fuel efficiency improvements [31]. Noteworthy research has delved into the influence of grain size on the intrinsic mechanical stability of austenite in TRIP steels [32], yet it has overlooked the impact of bainitic temperature. In contrast, another study concentrates on achieving ultra-high tensile strength in low-density δ-TRIP steels [33]. Despite effectively controlling δ-ferrite morphology and volume fraction, this research fails to examine the diverse processing conditions during the second stage of heat treatment and their ramifications for microstructural stability.

Recognizing these research efforts, a notable study has delved into the structure-property relationship in vanadium micro-alloyed TRIP steel, yielding valuable insights into microstructural evolution and mechanical properties within the realm of TRIP steel [34]. Nevertheless, despite these advancements, a noticeable gap remains in understanding the isothermal bainitic transformation (IBT) heat-treatment process specific to δ-TRIP steel micro-alloyed with Mo. An all-encompassing exploration of this aspect is paramount to unveil its intricate behavior. Thus, this research embarks on precisely this mission, focusing on attaining robust impact toughness in δ-TRIP steel, Fe-0.2C-1.2Mn-4Al (wt%), micro-alloyed with Mo through a two-step heat treatment. This study examines the effects of varying isothermal bainitic transformation (IBT) temperatures, thereby revealing insights into the connection between processing conditions and the stability of microstructural components, ultimately shaping the material's overall mechanical behavior.

2. Experimental

2.1 Material design

In a laboratory-scale vacuum induction-melting furnace operating at a frequency of 2500 HZ, micro-alloying δ-TRIP steel ingot with 0.30 Mo in a 5 kg melt was performed. Electro-slag refining (ESR) was used to remove S and P from the ingots. The result of an Optical emission spectrometer-based spectroscopic study (PMI MASTER SMART) on steel is shown in Table 1. Atomic absorption spectroscopy (AAS) was used to determine the quantity of Al.

As soon as the steel ingots were ready, hot rolling was completed. At a final rolling temperature (FRT) of 900°C, the steel was hot-rolled to a thickness of 10 mm after being heated to 1200°C and homogenized. After cooling to room temperature (RT) in the air, the as-hot-rolled sheet was cut into small pieces. Following that, a two-stage heating treatment was applied to the samples. The procedure outlined here is shown graphically in Figure. 1. This process consisted of austenitizing the steel, which was then followed by an isothermal bainitic transformation (IBT) process that was carried out at temperatures lower than the martensite-finish temperature (Mf).

The inter-critical-annealing heat treatment temperature (ICA) was achieved by heating at 750°C, 800°C, 820°C, and 850°C for 10 min and quenching in water. To select the initial heat treatment temperature, the microstructure was checked and then, 820°C was chosen. In a furnace, the samples were subjected to a temperature of 820°C for a period of 10 min. It has been shown that the samples include both austenite and ferrite microstructure.

After being withdrawn from the furnace, the samples were immediately submerged in a salt bath, including a mixture of KNO_3 and $NaNO_3$ in equal parts, that was heated to 350°C, 400°C, and 450°C for 10 min. After taking the samples out of the oven, they were taken outside to cool to room temperature. TR-3B, TR-4B, and TR-5B refer to samples of TR that were heat treated at 350°C, 400°C, and 450°C IBT temperatures for 10 min, respectively.

2.2 Experimental procedure

The samples that had been subjected to heat treatment were then cross-cut through the middle in a direction that was perpendicular to the long axis. The observations were performed in the portion that was located directly in the middle of the cross-section. The heat-treated samples were successively ground with 100, 200, 400, 600, 800, 1000, 1500, 2000, 2500, and 5000 grit SiC papers and polished with particle sizes of 5 m and 1.5 m diamond grinding paste so that the room temperature microstructures could be seen. The last step included etching the samples for a total of one minute in 2% Nital solution. As a result, the microstructure of the samples could be visible by a microscope, which could then be identified.

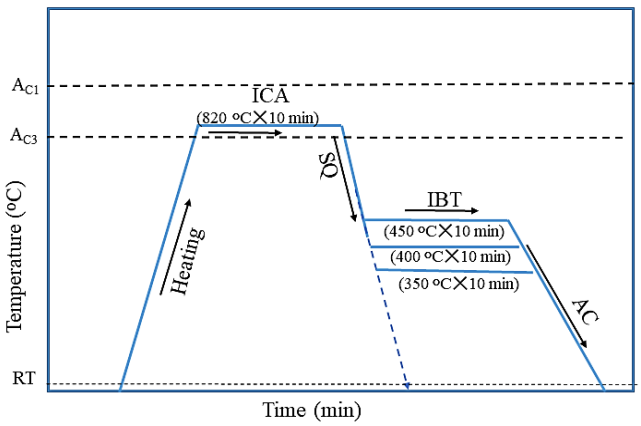

Figure. 1. Heat-treatment schematic for studied samples employing a practical, straightforward two-stage heat treatment procedure. AC is air cooling, SQ is salt quenching, and RT is room temperature.

Table 1. Chemical composition of experimental steels (wt%).

Sample	C	Al	Mn	Mo	Si	Nb	Cu	Ni	P	S	Fe
TR	0.22	3.90	1.12	**0.30**	0.48	0.002	0.02	0.030	0.011	0.009	Bal.

The concentration of C in the RA was determined by measuring the volume fraction (vol%) of the RA phase using X-ray diffraction (XRD) at room temperature using Cu (Cu-Kα) radiation (0.15402 nm). The samples were prepared in accordance with accepted practices in metallography. X-ray diffraction was used to scan the samples at a step rate of 0.04o/s across the range 2θ=10° to 100°. Integrating the intensities of the (200)α, (211)α, and (111)ɣ, (200) ɣ, and (220) ɣ peaks led to the calculation of the volume fraction of retained austenite (VRA) [35,36]. The formula is as follows (Equation (1)):

$$V_{RA} = \frac{1.4\, I_\gamma}{I_\delta + 1.4\, I_\gamma} \quad (1)$$

where Iγ is austenite's integrated intensity and Iδ is for phase.

To determine the C content in RA, the empirical equation (Equation (2)), in which XC, XAl, and XMn are the concentrations in wt% of C, Mn, and Al, respectively, were utilized. a is the austenite lattice parameter (Å). For simplicity, RA was considered to have the same alloying components as steel under all production conditions. The following calculation computed the average C content of RA in samples [37] (Equation (2)):

$$a_\gamma = 3.578 + 0.033X_C + 0.033X_{Al} + 0.033X_{Mn} \quad (2)$$

Additional investigation on the microstructure of the material was carried out with the assistance of an Olympus BX51 optical microscope (OM). In order to observe the microstructure of the samples in greater detail, the surface of the etched samples was photographed using a Field emission scanning electron microscope (FE-SEM/ TESCAN MIRA3) at magnifications of 5000 times and 10000 times. This allowed for a more in-depth examination of the samples' internal composition.

Tensile testing, according to ASTM E8, was utilized to analyze the mechanical properties of the hot-rolled and heat-treated samples. The samples were cut from the hot-rolled steels in the direction of rolling using a waterjet machine. The longitudinal axis of the tensile specimens was machined to be parallel to the direction of rolling. Dimensions of samples are displayed in Figure 2, measured 25 mm in length, 10 mm in width, and 4 mm in thickness. The 50000 N load range MTS universal testing machine was used for the tensile test, which was conducted at room temperature with a crosshead speed of 0.3 mm·min^{-1}. At least two samples were analyzed in each condition.

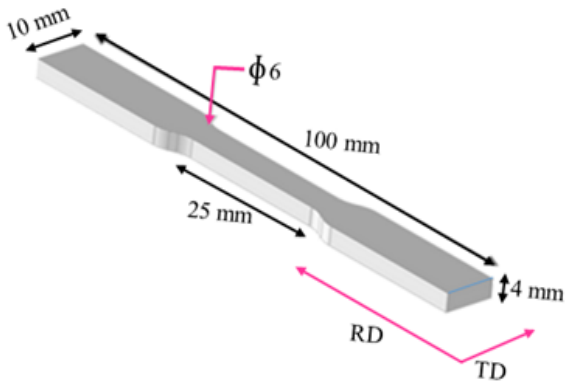

Figure 2. The geometry of the tensile test specimen.

3. Results and discussion

3.1 The Phase transformation behavior

The equilibrium phase fraction that was computed by ThermoCalc software with the TCFE9 database for alloy TR as a function of temperature can be seen in Figure 3. This area has been subjected to the presence of metal melt (L), ferrite (F), austenite (A), and cementite (C).

Since Al content is up to 4 wt%, Figure 3(a) shows a single ferrite range. Al stabilizes the phase diagram's δ-ferrite phase. Al, like Si and P, does not dissolve in carbide, slowing Fe_3C formation [15,38]. Importantly, high Al concentration may produce and stabilize δ-ferrite in steel [25]. However, adding a considerable amount of Mn improves the ferrite and austenite range. Cementite shows a lower critical temperature. The investigated steel has Mn content of around 1.2 wt%, which is the minimum required for increased hardness above typical steel [1]. Austenite can be stabilized if the temperature at which Fe_3C begins to form can be decreased, allowing austenite to form.

According to Figure 3, the first phase that nucleates and develops out of the metal melt is δ-ferrite. This phase may be found in the solid state. The only solid phase till the melt is used up is δ-ferrite. According to the microstructures of TR sample, the fraction of ferrite that is at its lowest is around 58%. The liquid cannot become austenite until it turns into δ-ferrite. During non-equilibrium cooling, the elemental separation in the interdendritic zones may trend towards the melt's local chemical composition, especially in the last stage of solidification. Thus, the liquid may include alloy components in the final solidification zone. Cooling is more probable in an unstable condition while all diagrams are formed in an equilibrium state. Austenite grows as δ-ferrite is consumed during cooling. When ferrite surpasses the minimum volume fraction, austenite transforms into α-ferrite or pearlite, a different shape from dendritic-ferrite. Based on the phase diagram, the alloy cannot have complete austenite at any temperature.

The temperature at which cementite dissolves is about 550°C. RA is expected to reach a maximum of 50% when the steel is cooled from the intercritical temperature of 1000°C. Athermal martensite arises during cooling because austenite has much lower thermal stability than martensite below 1000°C and higher annealing temperatures. Figure 3 calculated the standard finish temperature of the transition from ferrite and Fe_3C to austenite to be between 550 and 560°C.

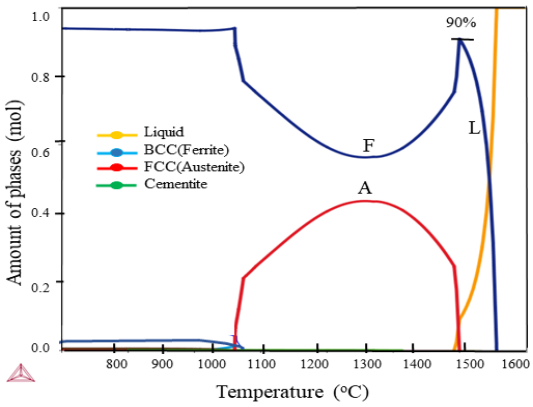

Figure 3. Analyzed equilibrium phase fraction vs temperature by ThermoCalc software for the tested steel. (Calculations were performed using the TCFE9 database from ThermoCalc).

3.2 Effect of Mo-alloy and IBT time on microstructure evolution

3.2.1 XRD studies

The XRD pattern of sample TR in its as-rolled form, termed TR-A, is shown in Figure 4. As can be seen very well in Figure 4, the ferrite is present in the final product.

Upon analysis of the XRD pattern, it is apparent that BCC (δ-ferrite) is seen in the as-rolled condition. It is worth noting that a single peak corresponding to austenite has been observed. This discovery implies that the role of this phase in the transformation into martensite during mechanical testing is negligible. The XRD findings confirm the significant concentration of aluminum, highlighting the persistence of BCC (δ-ferrite) during the hot-rolling procedure.

In order to get a deeper understanding of the role that austenite and bainite play in the process of enhancing TRIP characterization, the effect of IBT temperature in 10 min through a two-step heat treatment was explored. In this study, XRD analysis was performed in order to explore and precisely identify the different kinds of phases, as well as the volume fraction of RA and the amount of C in RA. Samples were exposed to different IBT temperatures, and their diffraction patterns are displayed in Figure 5. The discrepancies in VRA and C content of RA between the samples are analyzed in detail in Table 2.

Figure. 5 shows that heat-treated steels have BCC (δ-ferrite) and FCC (RA) phases in their microstructures. Because TRIP steels' mechanical properties rely on RA, optimizing their microstructure is critical. Thus, increasing the volume fraction of RA phase and C content of TRIP steel improves its mechanical characteristics.

As a result of the change from ferrite to austenite that takes place during the process of heat treatment, the peaks of the austenite become more intense and more distinct after the treatment.

Yi *et al*. [20] have observed that the solid-state transition of the ferrite into the austenite that occurs during further heat treatment and hot rolling causes the consumption of the ferrite. Even after the hot rolling process, the existence of the ferrite was seen in this investigation because of the significant quantities of Al and Si. The results of the XRD test proved this. Choi *et al*. [38] revealed that the cooling rate and chemical composition affect the existence of ferrite in the microstructure. Slow cooling consumes more δ-ferrite and acts similarly to hot rolling.

The volume fractions of austenite in samples TR-B3, TR-B4, and TR-B5 were computed and it was about 27%, 24% and 22%, respectively, at 350°C, 400°C and 450°C, as shown in Table 2. This result demonstrates that the chosen quantity of Al, as well as other realistic factors, would result in stable δ-ferrite in both samples under three circumstances. Steel A has a maximum RA content after holding in 10 min at 350°C IBT temperature, where both forms of RA work together to increase resistance to mechanical deformation, creating a cumulative and persistent TRIP effect. The elevated volume fraction of RA in sample TR-3B is due to austenite stabilization by saturation with C rejected from neighboring produced bainite laths.

It is well-recognized that the high C content in RA is due to the rejection of C atoms from nearby grains during the IBT process [5,7]. This is the reason for the high C content of RA. Because the sheaf type of RA has a broad interface but a short diffusion route, the C atoms might diffuse more quickly from the grains that are nearby to the sheaf type of RA. The disparity in C content has the potential to influence the Ms and, as a consequence, the austenite's stability. As a result, the untransformed austenite has a larger concentration of C as compared to the majority of the alloy.

Once the isothermal hold temperature was lowered from 450°C to 350°C, steel's VRA increased noticeably. Since carbides tend to form easily at such temperature, C precipitates as carbide in the thin layers that make up bainitic ferrite plates, making less of it available for the stabilisation and retention of RA. The sample has the lowest VRA at 450°C. Nevertheless, Pourfarokh *et al*.[21] found that VRA at 450°C was best for the steel with a little lower Mo content (0.05 wt%). The use of IBT over a shorter period of time (i.e., 10 versus 6 min) is one element among several that may account for this difference.

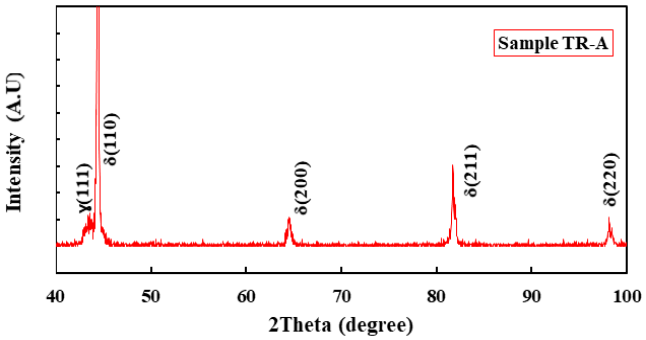

Figure 4. XRD pattern of TR-A (as-rolled sample).

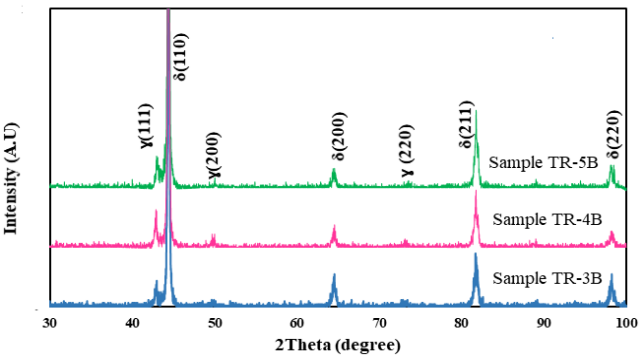

Figure 5. XRD patterns for TR-3B, TR-4B, and TR-5B samples.

Table 2. Measured RA of heat-treated samples at different IBT temperatures.

Sample	ICA temperature (°C)	IBT time (min)	IBT temperature (°C)	IBT time (min)	Carbon content (wt%)	Retained austenite (V%)
TR-3B	820	10	350	10	1.45	27
TR-4B	820	10	400	10	1.40	24
TR-5B	820	10	450	10	1.38	22

On the other hand, if they both had the same C content, we would expect them to have the same RA and, by extension, the same stabilising effect. Mo may also have a strong impact on the solid solution strengthening, which would make it possible for it to act as a physical barrier against the premature transformation of RA to martensite.

The maximum amount of C is present in RA at an isothermal temperature of 350°C. When the temperature of the bainite transition increases, C concentration falls. IBT inhibits carbide formation, leading to C enrichment, because of high Al in steel's chemical composition.

3.2.2 Optical and FE-SEM studies

In Figure 6, the optical pictures at different magnifications of the investigated steels with three different IBT temperatures are shown. These steels were heat-treated at 10 min of IBT time. Multi-phase structures of δ-ferrite, α-ferrite, ferritic bainite, and RA/martensite (A/M) have developed and been identified in OM images in all of the samples. Secondary phases that occur in the rolling direction are identified in the OM pictures as α-ferrite, ferritic bainite, and A/M phases. The coarse δ-ferrite remained stable following the two-step heat treatment. The presence of δ-ferrite can be attributed to the high Al content, which is a strong δ-ferrite phase stabilizer [20,38,39]. The distinction between δ-ferrite and α-ferrite may be made by classifying them as follows: α-ferrite is the product of the transformation of austenite by ICA, whereas δ-ferrite originates from solidification and survives through hot deformation [40].

The austenite phase was transformed into the bainitic ferrite phase following heat treatment at IBT temperature. As can be seen, when IBT temperature increase, the sheaf structure of A/M in secondary phases changes to a blocky structure, and the amount of sheaf bainite increases.

According to other studies [38,41], the microstructure of the samples without the second stage of heat treatment is mostly composed of lath martensite or martensite/austenite (M/A), and α-ferrite in δ-ferrite matrix. Further, IBT treatment at 450°C for 10 min might significantly reduce the martensite or M/A components' fractions and generate lath-like bainitic ferrite, α-ferrite, and RA phases. However, it is nearly impossible to recognize the distinction between martensite and M/A constituents in FE-SEM images. After etching, the ferrites (δ, α, and αb) undergo deeper etching than the austenite phase [42].

Isothermal heat-treated samples (shown as pictures in Figure 7) were analyzed using field-emission scanning electron microscopy (FE-SEM). As a consequence, in the FE-SEM micrographs of δ-TRIP steels shown in Figure 7(a-c), the RA phase is bright and the ferrite phase is dark. Furthermore, the morphologies of bainitic and α-ferrite can be distinguished. α-ferrite has an equiaxed morphology, as opposed to bainitic ferrite, which has a lamellar structure within RA phase plates. All these phases are laballed in the FE-SEM pictures. The high resolution of FE-SEM images are shown in Figure 7(a2, b2, and c2), in order to make the microstructures' finer features clearer. These photos show that two different kinds of blocky and lamellar morphology for the RA phase developed in the samples. Because austenite is sufficiently stable, δ-TRIP alloys made of lath RA may exhibit improved ductility.

It has been hypothesized that the bainite transformation ceased and blocky austenite was retained after the composition of austenite approached the T'0 curve during the IBT phase of heat treatment [43,44]. In this second stage of heat-treatment, the remaining blocky austenite from the first step may be refined, which increases its stability. As a result, the IBT process results in a stronger and more carbon-rich lath austenite phase [43,45]. Using an IBT step of heat treatment at 350°C, 400°C, and 450°C for 10 min, lath austenite is formed in sample TR-A. (Figure 7(a-b)). The majority of the austenite morphology in sample TR- B5 in Figure 7(c) seems to be blocky in contrast to Figure 7(a) in sample TR-B3. As a result, when the holding temperature at IBT is extremely low, the development of a lath-shaped kind of bainitic ferrite is feasible. The findings here agree with those of Pourfarokh *et al*.[21].

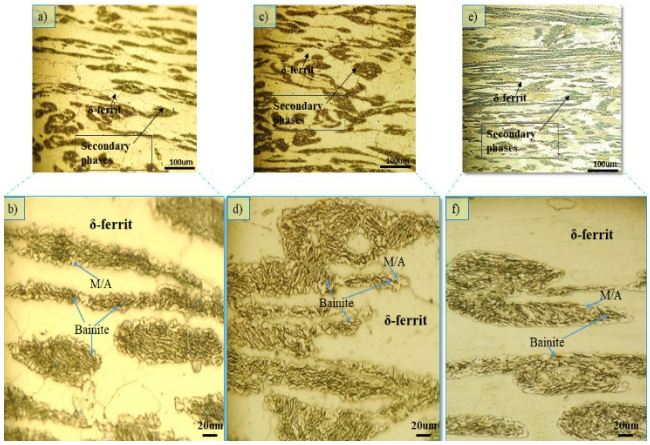

Figure. 6. Optical microscopy of samples: (a and b) TR-3B, (c and d) TR-4B, and (e and f) TR-5B. M: martensite, RA: retained austenite.

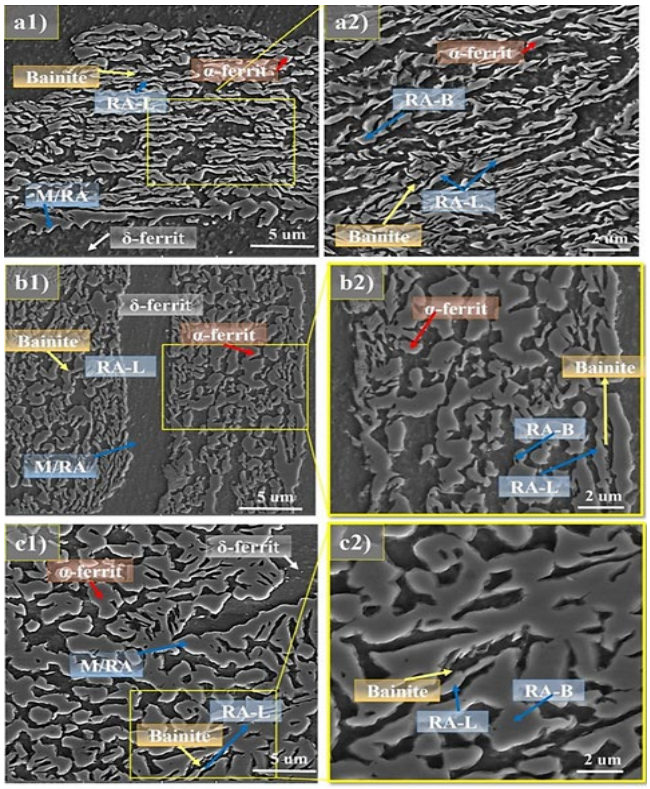

Figure 7. FE-SEM micrograph of samples: (a1 and a2) TR-3B, (b1 and b2) TR-4B, and (c1 and c2) TR-5B. M: martensite, RA: retained austenite.

Seeing the samples, it is clear that when IBT temperature drops, the bainite undergoes a structural transition from coarse to fine lath. Hanzaki *et al*. [46] found that color etching can identify the RA from the other phases, even while 2% Nital etching does not display the RA and martensite phases.It has been proven by Hanzaki *et al*. that color etching is highly successful in identifying the RA from the other phases, even though the RA and martensite are not clearly apparent by the etching method used (i.e. 2% Nital solution). His research has shown that at 500°C, the RA is surrounded by thick ferritic platelets, whereas at the lower temperature (i.e. 300°C), RA is primarily imprisoned between laths of bainitic ferrite. However, it doesn't seem that the vicinity of these two phases, each of which has a distinct strength, is a good combination of mechanical characteristics.

3.3 Mechanical properties

The Mo micro-alloyed δ-steel underwent two-stage heat treatment at a range of IBT temperatures (350°C, 400°C, and 450 °C). Results for yield strength (YS), ultimate tensile strength (UTS), and total elongation (TE) values for the as-annealed sample (TR-A) are shown in Table 3. Figure 8 shows the engineering stress-strain curves of the experimental steels at different IBT temperatures. Moreover, the results of YS, UTS, TE and the product of strength and elongation (PSE) are provided in Table 4 for samples TR-3B, TR-4B and TR-5B.

When secondary phases are allowed to develop, steel's mechanical properties are transformed. Data analysis of Tables 3 and Table 4 shows that heating the samples improved their overall strength. Both the tensile and yield strengths of δ-TRIP steel are significantly affected by the volume fraction of bainite. Changes in martensite composition and RA stability in heat-treated samples might account for the observed difference in YS and UTS with increasing IBT temperature (Figure 8). In engineering stress-strain curves, the yielding behaviour is proven to be continuous. During the ICA phase, austenite has a higher solubility for C than ferrite. Serrations in stress-strain curves were therefore avoided for all specimens as a result of the two-step heat treatment, which raised C in RA while lowering C in ferrite. Martensite generated by strain-induced austenite/martensite transition may also create moveable dislocations at the ferrite/martensite interface, which may contribute to continuous yielding behavior [47].

The stability of RA makes the material more ductile while simultaneously increasing its strength thanks to the TRIP effect. After experiencing the ICA step for 10 min at 820°C, the samples were subjected to an IBT for 10 min at 350°C, 400°C, and 450°C.

As a result, bainite developed, increasing the quantity of RA in the material. Steel displays a rise in its UTS as IBT temperature is decreased (Table 4), which is primarily in part owing to the fact that steel has a finer structure overall [27,48]. The tensile properties of sample TR-3B (about 860 MPa UTS and 41% TE) are enhanced due to the development of fine bainitic structure and RA for 350°C of IBT step. However, for sample TR-4B, these figures were 854 MPa and 33% at an IBT temperature of 400°C. At 450°C during the IBT process, the tensile strength of the sample TR-5 is about 850 MPa (Table 4). As compared to what Poorfarokh *et al*. and Hanzaki *et al*. observed, the UTS results for the TRIP steels are much lower. This drop in tensile strength might be attributed to somewhat lower Mo content and other hot-rolling-related issues. Elongation, on the other hand, provided results that were within the range obtained by the previous authors.

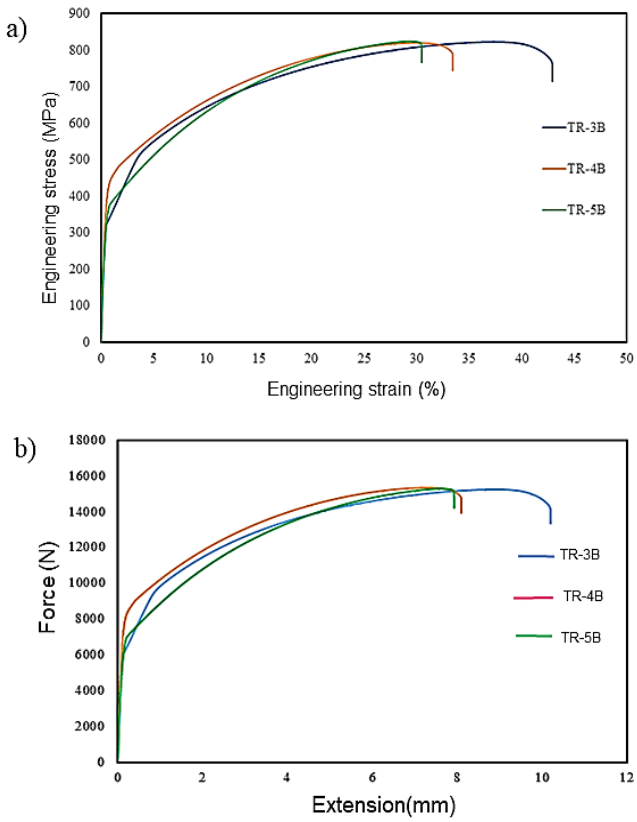

Figure. 8. Mechanical properties of samples TR-3B, TR-4B, and TR-5B, a) Engineering stress-strain curves, and b) Force- extension curves.

Table 3. Mechanical properties of TR-A sample.

Sample	Mo-alloy (wt%)	Condition	Maximum force (N)	YS (0.2% MPa)	UTS (MPa)	TE (%)	PSE (MPa·%)
TR-A	0.30	As-rolled	14240	400	800	21	16800

Table 4. Mechanical properties of the studied samples at different IBT temperatures.

Sample	ICA temperature (°C)	ICA time (min)	IBT temperature (°C)	IBT time (min)	Maximum force (N)	YS (0.2%MPa)	UTS (MPa)	TE (%)	PSE (MPa.%)
TR-3B	820	10	350	10	15308	500	860	41	35260
TR-4B	820	10	400	10	15201	430	854	33	28182
TR-5B	820	10	450	10	15130	400	850	32	27200

The retained low C content austenite does not improve TRIP steel's formability since it transforms into martensite at moderate loads. A high-carbon type of austenite is retained throughout the deformation process and only partially transforms into martensite. Because of this, it doesn't provide much in the way of ductility improvement. Thus, modifying the C content of RA is necessary to enhance the mechanical characteristics of TRIP steels.

At 350°C, steel achieves its maximum VRA, which is also its maximum ductility. As was mentioned previously in this article, the large elongation measures exhibited are the result of the higher VRA and the wide range of stability levels that may be produced at this temperature.

Since RA phase is predominantly responsible for plastic deformation in these materials, a drop in the austenite phase fraction may lead to a reduction in elongation [33,44]. This meant that elongation for TR-5B was 32%.

Both the size and shape of retained austenite affect its stability. When comparing the two types of RA, lamellar and fine retained austenite are more stable. RA is transformed into martensite under low stress due of its low C enrichment and enormous size. Highest overall elongation is seen in lamellar RA in the microstructure of δ-TRIP steels.

As the temperature of the IBT is decreased, the results of the mechanical properties demonstrate that there is a rise in its YS. The high resistance of the RA to mechanical deformation may be due to the combined effect of Mo's solid solution strengthening and the action of C. TR-3B with the greatest volume content and the most stable RA had the highest PSE (35260 MPa·%), which is a measure of the amount of energy absorbed throughout the deformation process. It was subjected to heat treatment at an isothermal temperature of 350°C.

All of this illustrates that ultrafine heterogeneous structures may be generated by thermomechanical processing, and that these structures have the potential to give extraordinary mechanical qualities.

4. Conclusions

In this work, the RA stability of δ-TRIP steel was evaluated after being subjected to a variety of IBT temperatures. The following is an outline of the most significant results from the investigation:

1) The findings from the XRD analysis verify the existence of δ-ferrite as well as RA in the microstructure of the steel that was investigated. The microstructure of examined δ-TRIP-assisted steel, has δ-ferrite, α-ferrite, bainitic ferrite, martensite, and RA.

2) Within the microstructure of the investigated steel, RA emerged with both a blocky and a lamellar morphology. The volume fraction of RA has increased to around 22% to 27% after completing two stages of heat-treatment.

3) Sample TR-3B (0.2%C-4%Al-1.5%Mn-0.3%Mo) was found to have the highest PSE (35260 MPa·%) and maximum Gelongation (41%) after being heat-treated at 350°C. Tensile strength was highest in this sample (860 MPa).

4) The circumstances under which these steels are processed have a direct impact on their mechanical properties (i.e, IBT temperature). In this way, it has been shown that an increase in IBT temperature results in a decrease in strength and total elongation. In contrast, the results of other research contradict this conclusion. There could be additional factors involved.

5) The microstructure has a significant impact on the strength, while the microstructure and V_{RA} both have a significant impact on the total elongation. At IBT temperature of 350°C, the volume fraction of RA reaches a maximum of 27%, and PSE surpasses 35 GPa·%.

References

[1] D. K. Matlock, and J. G. Speer, "Processing opportunities for new advanced high-strength sheet steels," *Materials Science and Technology,* vol. 25, no. 1-3, pp. 7-13, 2010.

[2] H. Yi, "Review on δ-transformation-induced plasticity (TRIP) steels with low density: the concept and current progress," *JOM,* vol. 66, no. 9, pp. 1759-1769, 2014.

[3] C. Liu, Q. Peng, and Z. Xue, "Microstructure and mechanical properties of Mo-Nb microalloyed medium Manganese trip steel by cyclic quenching," *Metallurgical and Materials Engineering,* vol. 25, no. 2, pp. 139-146, 2019.

[4] J. Chiang, J. Boyd, A. J. M. S. Pilkey, and E. A, "Effect of microstructure on retained austenite stability and tensile behaviour in an aluminum-alloyed TRIP steel," *Materials Science and Engineering: A*. vol. 638, pp. 132-142, 2015.

[5] E. Parker, and V. J. E. f. m. Zackay, "Enhancement of fracture toughness in high strength steel by microstructural control," *Engineering Fracture Machanics,* vol. 5, no. 1, pp. 147-165, 1973.

[6] O. Matsumura, Y. Sakuma, and H. TakeChi, "Enhancement of elongation by retained austenite in intercritical annealed 0.4 C-1.5 Si-O. 8Mn Steel," *Transactions of the Iron and Steel Institute of Japan,* vol. 27, no. 7, pp. 570-579, 1987.

[7] S. Traint, A. Pichler, M. Blaimschein, B. Röthler, C. Krempaszky, and E. Werner, "Alloy design, processing and properties of TRIP-steels: A critical comparison," in *International. Conference on Advanced High-Strength Sheet Steel for Automotive Applications*, 2004, pp. 79-98.

[8] K.-i. Sugimoto, and A. K. Srivastava, "Microstructure and mechanical properties of a TRIP-aided martensitic steel," *Metallography, Microstructure, Analysis,* vol. 4, no. 5, pp. 344-354, 2015.

[9] B. Hance, "Advanced high strength steel: Deciphering local and global formability," in *Proc. International Automotive Body Congress, Dearborn, MI*, 2016.

[10] A. Haldar, S. Suwas, and D. Bhattacharjee, *Microstructure and Texture in Steels: and Other Materials*. Springer, 2009.

[11] F. Zhang, X. Long, J. Kang, D. Cao, B. J. M. Lv, and Design, "Cyclic deformation behaviors of a high strength carbide-free bainitic steel," *Materials & Design,* vol. 94, pp. 1-8, 2016.

[12] J. Chiang, B. Lawrence, J. Boyd, A. J. M. S. Pilkey, and E. A, "Effect of microstructure on retained austenite stability and work hardening of TRIP steels," *Materials Science and Engineering: A*, vol. 528, no. 13-14, pp. 4516-4521, 2011.

[13] R. Ranjan, H. Beladi, P. D. Hodgson, and S. B. Singh, "The Mechanical Properties of Low Alloy TRIP-Aided Steel: The Role of Retained Austenite," *Metallurgical Materials Transactions A,* vol. 52, no. 10, pp. 4649-4663, 2021.

[14] X. Kai, C. Chen, X. Sun, C. Wang, and Y. Zhao, "Hot deformation behavior and optimization of processing parameters of a typical high-strength Al–Mg–Si alloy," *Materials & Design,* vol. 90, pp. 1151-1158, 2016.

[15] P. Jacques, P. Harlet, and F. Delannay, "Critical assessment of the phase transformations occuring during the heat-treatment of TRIP-assisted multiphase steels," in *International Conference on TRIP-aided high strength ferrous alloys*, 2002.

[16] Y. Sakuma, O. Matsumura, and H. Takechi, "Mechanical properties and retained austenite in intercritically heat-treated bainite-transformed steel and their variation with Si and Mn additions," *Metallurgical Transactions A,* vol. 22, no. 2, pp. 489-498, 1991.

[17] R. Karami, and M. A. A. J. P. o. t. I. o. M. E. Abdollahi, "Mechanical and corrosion characteristics of 6061–T6 aluminum alloy samples reinforced with alumina micro and nanoparticles fabricated by friction stir processing," *Part C: Journal of Mechanical Engineering Science,* vol. 237, no. 16, pp. 3587-3596, 2023.

[18] S. Chatterjee, M. Murugananth, and H. Bhadeshia, "δ TRIP steel," *Materials Science and Technology,* vol. 23, no. 7, pp. 819-827, 2007.

[19] H. Yi, K. Lee, and H. Bhadeshia, "Extraordinary ductility in Al-bearing δ-TRIP steel," *Proceedings of the Royal Society A: Mathematical, Physical Engineering Sciences,* vol. 467, no. 2125, pp. 234-243, 2011.

[20] H. Yi, K. Lee, and H. Bhadeshia, "Mechanical stabilisation of retained austenite in δ-TRIP steel," *Materials Science and Engineering: A,* vol. 528, no. 18, pp. 5900-5903, 2011.

[21] A. Pourfarokh, H. Jafarian, A. Eivani, Y. Palizdar, and N. Park, "Regulating tensile properties through bainitic transformation temperature in a hot-rolled δ-TRIP steel," *Materials Science Technology,* vol. 36, no. 2, pp. 223-232, 2020.

[22] D. Yang, P. Du, D. Wu, H. J. J. o. M. S. Yi, and Technology, "The microstructure evolution and tensile properties of medium-Mn steel heat-treated by a two-step annealing process," vol. 75, pp. 205-215, 2021.

[23] W. Ding, P. Hedström, and Y. Li, "Heat treatment, micro-structure and mechanical properties of a C–Mn–Al–P hot dip galvanizing TRIP steel," *Materials Science and Engineering: A,* vol. 674, pp. 151-157, 2016.

[24] C.-Y. Chen and M.-H. Liao, "Synergistic effects of carbon content and Ti/Mo ratio on precipitation behavior of HSLA steel: Insights from experiment and critical patent analysis," *Materials & Design,* vol. 186, p. 108361, 2020.

[25] S. D. Nath,, E. Clinning, G. Gupta, V. Wuelfrath-Poirier, G. L'Esperance, O. Gulsoy, M. Kearns, and S. V. Ttre, "Effects of Nb and Mo on the microstructure and properties of 420 stainless steel processed by laser-powder bed fusion," *Additive Manufacturing,* vol. 28, pp. 682-691, 2019.

[26] K.-i. Sugimoto, S.-h. Sato, J. Kobayashi, and A. K. Srivastava, "Effects of Cr and Mo on mechanical properties of hot-forged medium carbon TRIP-aided bainitic ferrite steels," *Metals,* vol. 9, no. 10, p. 1066, 2019.

[27] M. Bouet, J. Root, E. Es-Sadiqi, and S. Yue, "The effect of Mo in Si-Mn Nb bearing TRIP steels," in *Materials science forum*, 1998, vol. 284, pp. 319-326: Trans Tech Publ.

[28] A. Kozłowska, K. Radwański, K. Matus, L. Samek, A. J. A. o. C. Grajcar, and M. Engineering, "Mechanical stability of retained austenite in aluminum-containing medium-Mn steel deformed at different temperatures," *Archives of Civil and Mechanical Engineering*, vol. 21, no. 1, pp. 1-15, 2021.

[29] M. Xia, Z. Tian, L. Zhao, and Y. N. Zhou, "Fusion zone microstructure evolution of Al-alloyed TRIP steel in diode laser welding," *Materials transactions,* vol. 49, no. 4, pp. 746-753, 2008.

[30] H. Townsend, "Effects of silicon and nickel contents on the atmospheric corrosion resistance of ASTM A588 weathering steel," *American Society for Testing and Materials, Philadelphia*, vol. 1239, pp. 85-85, 1995.

[31] D.-W. Suh, and S.-J. J. S. M. Kim, "Medium Mn transformation-induced plasticity steels: Recent progress and challenges," *Scripta Materialia*, vol. 126, pp. 63-67, 2017.

[32] D. P. Yang, T. Wang, Z. T. Miao, P. J. Du, G. D. Wang, and H. L. Yi, "Effect of grain size on the intrinsic mechanical stability of austenite in transformation-induced plasticity steels: The competition between martensite transformation and dislocation slip," *Journal of Materials Science & Technology*, vol. 162, pp. 38-43, 2023.

[33] G. Q. Li, Y. F. Shen, N. Jia, X. W. Feng, and W. Y. Zue, "Microstructural evolution and mechanical properties of a micro-alloyed low-density δ-TRIP steel," *Materials Science and Engineering: A.,* vol. 848, p. 143430, 2022.

[34] J. Lu, S. Wang, H, Yu, G. Wu, J. Gao, H. Wu, H. Zhao, C. Zhang, and Z. Mao, "Structure-property relationship in vanadium micro-alloyed TRIP steel subjected to the isothermal bainite transformation process," *Materials Science and Engineering: A.* vol. 878, p. 145208, 2023.

[35] A. Grajcar, H. J. J. o. A. i. M. Krztoń, and M. Engineering, "Effect of isothermal bainitic transformation temperature on retained austenite fraction in C-Mn-Si-Al-Nb-Ti TRIP-type steel," *Thermaldynamics,* vol. 35, no. 2, pp. 169-176, 2009.

[36] A. K. Srivastava, G. Jha, N. Gope, and S. J. M. C. Singh, "Effect of heat treatment on microstructure and mechanical properties of cold rolled C–Mn–Si TRIP-aided steel," *Materials Characterization*, vol. 57, no. 2, pp. 127-135, 2006.

[37] N. Van Dijk, A. M. Butt, L Zhao, J. Sietsma, S. E. Offerman, J. P. Wright, and S. van der Zwaag, "Thermal stability of retained austenite in TRIP steels studied by synchrotron X-ray diffraction during cooling," *Acta Materialia*, vol. 53, no. 20, pp. 5439-5447, 2005.

[38] Y. J. Choi, D.-W. Suh, and H. Bhadeshia, "Retention of δ-ferrite in aluminium-alloyed TRIP-assisted steels," *Proceedings of the Royal Society A: Mathematical, Physical and Engineering Sciences,* vol. 468, no. 2146, pp. 2904-2914, 2012.

[39] H. Yi, S. Ghosh, W. Liu, K. Lee, and H. Bhadeshia, "Non-equilibrium solidification and ferrite in δ-TRIP steel," *Materials Science and Technology,* vol. 26, no. 7, pp. 817-823,

[40] Y. Palizdar, R. Cochrane, R. Brydson, F. Bygrave, and A. Scott, "Understanding the role of aluminium in low level nitrogen steels via microstructural characterisation," in *Journal of Physics: Conference Series*, 2008, vol. 126, no. 1, p. 012019: IOP Publishing.

[41] S. G. Shiri, S. A. J. Jahromi, Y. Palizdar, and M. Belbasi, "Unexpected effect of Nb addition as a microalloying element on mechanical properties of δ-TRIP Steels," *Journal of Iron and Steel Research International,* vol. 23, no. 9, pp. 988-996, 2016.

[42] K.-i. Sugimoto, M. Murata, T. Muramatsu, and Y. Mukai, "Formability of C–Si–Mn–Al–Nb–Mo ultra high-strength TRIP-aided sheet steels," *ISIJ international,* vol. 47, no. 9, pp. 1357-1362, 2007.

[43] H. D. H. Bhadeshia, and D. Edmonds, "The bainite transformation in a silicon steel," *Metallurgical Transactions A,* vol. 10, no. 7, pp. 895-907, 1979.

[44] H. Bhadeshia, and R. Honeycombe, *Steels: microstructure and properties*. Butterworth-Heinemann, 2017.

[45] H. Bhadeshia, and R. Honeycombe, "Steels: microstructure and properties. 2006," *BH Pub,* pp. 42-44.

[46] A. Z. Hanzaki, H. PD, and S. Yue, "The influence of bainite on retained austenite characteristics in Si-Mn TRIP steels," *ISIJ international,* vol. 35, no. 1, pp. 79-85, 1995.

[47] S. Kim, Y. Kim, Y. Lim, and N. J. Kim, "Relationship between yield ratio and the material constants of the swift equation," *Metals Materials International,* vol. 12, pp. 131-135, 2006.

[48] A. Zarei-Hanzaki, "Transformation characteristics of Si-Mn TRIP steels after thermomechanical processing," *Canada: McGill University,* 1994.